First Observation of Alpha Particle Loss Induced by Kinetic Ballooning Modes in TFTR Deuterium-Tritium Experiments

Zuoyang Chang,[1] R. V. Budny,[1] L. Chen,[2] D. Darrow,[1] E. D. Fredrickson,[1] A. Janos,[1] D. Mansfield,[1] E. Mazzucato,[1] K. M. McGuire,[1] R. Nazikian,[1] G. Rewoldt,[1] J. D. Strachan,[1] W. M. Tang,[1] G. Taylor,[1] R. B. White,[1] S. Zweben,[1] and TFTR Group

[1]*Plasma Physics Laboratory, Princeton University, Princeton, New Jersey 08543*
[2]*Department of Physics, University of California, Irvine, California 92717-4575*

A correlation between the measured alpha particle loss and high frequency ($\sim 100-200$ kHz) magnetohydrodynamic (MHD) modes has been observed in some high β (= plasma pressure/magnetic pressure) DT plasmas in TFTR. These modes are localized around the peak plasma pressure gradient and have ballooning characteristics. Particle simulation shows that the loss is due to wave-particle resonances. Linear instability analysis indicates that the plasma is unstable to the kinetic MHD ballooning modes driven by strong local pressure gradients.

Study of MHD effects on alpha particle confinement is one of the most important subjects in the recent deuterium-tritium (DT) fusion research in the Tokamak Fusion Test Reactor (TFTR). It has been theoretically predicted [1] that energetic alpha particles ($E_\alpha \lesssim 3.5$ MeV) can either drive or resonate with plasma MHD fluctuations. This kind of wave-particle interaction can induce direct alpha particle loss and therefore has an important impact on tokamak fusion devices.

In a recent high β, high power DT experiment [2], good correlation was found between high frequency MHD modes and the measured alpha losses. A detailed study of the high frequency MHD modes in normal TFTR supershot plasmas can be found in Ref. [3]. This paper will focus on the first observation of the alpha particle losses correlated with these modes.

Figure 1 shows one of the highest performance discharges achieved using intensive lithium wall conditioning [2]. Some measured parameters are (in conventional notation) $I_p = 2.1$ MA, $B_t = 5.1$ T, $P_B = 21$ MW, $R = 2.52$ m, $a = 0.87$ m, $q_a \simeq 4.6$, $\tau_E \simeq 0.28$ sec, $T_i(0) \simeq 38$ keV, $T_e(0) \simeq 12$ keV, $n_e(0) \simeq 8.2 \times 10^{19}$ m^{-3}, $P_{\text{fusion}} \simeq 5.5$ MW, $\beta_N \simeq 1.7$. Large bursts of alpha loss as well as large fluctuations in the lost-alpha signal are observed around the peak performance phase as shown in Fig. 1(c). The alpha loss is measured by a detector located at the bottom of the limiter chamber (90° detector) [4]. It is found that these bursts (at $t = 4.3, 4.4$, and 4.46 sec) correspond to bursts of the high frequency MHD modes and lead to a performance degradation (for details, see Ref. [2]). This discharge suffered a high-β minor disruption at 4.55 sec, which terminated the enhanced confinement phase. This indicates that the plasma was near the beta limit. The high frequency MHD modes are observed at the peak performance phase ($t = 4.20-4.55$ sec). They are detected by the multichannel electron cyclotron emission (ECE) poly-

chromator arrays [5] and by the external magnetic probes [6]. According to their different characteristics, the high frequency modes can be further divided into two different modes in this discharge. One is the multifrequency quasicontinuous mode observed during the burst of alpha loss, e.g., the t_1 window in Fig. 1. The other one is the bursting (or intermittent) mode observed between the alpha bursts, e.g., the t_2 window in Fig. 1.

(1) Multifrequency quasicontinuous modes.— Figure 2(a) shows the contour plot of the frequency spectrum of δT_e measured from an ECE channel ($R \simeq 300$ cm or $r/a \simeq 0.34$). Multifrequency quasicontinuous modes with frequency up to 250 kHz are observed. The toroidal mode numbers $n \leq 7$ are measured from the magnetic coils. The rest are extrapolated based on the frequency spacing of the modes. The burst of these modes correlates with an enhancement of a factor
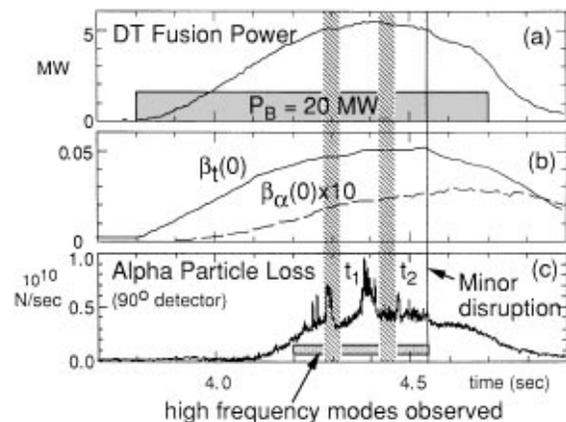

FIG. 1. A high-β DT discharge. (a) DT fusion power; (b) central total plasma beta $\beta_t(0)$ and the central alpha β; and (c) measured alpha particle loss rate. The high frequency modes developed in the time window are indicated. Different characteristics observed at different time (e.g., t_1 and t_2).
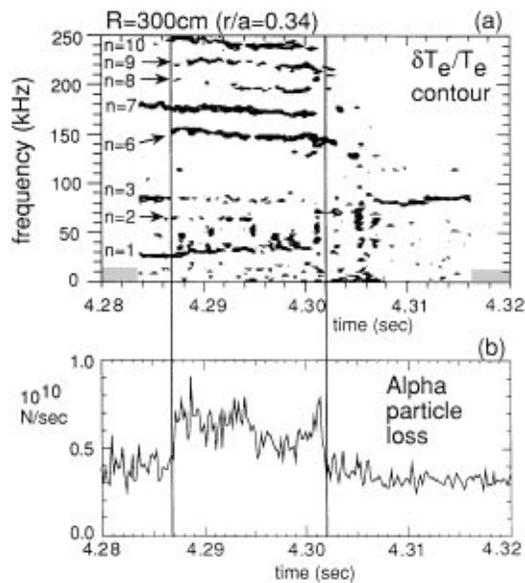
FIG. 2. Multifrequency quasicontinuous modes observed at the time t_1 in Fig. 1. (a) Frequency spectrum contour plot of $\delta T_e/T_e$ (at $R \simeq 300$ cm). (b) Alpha-loss signal from the 90° detector.
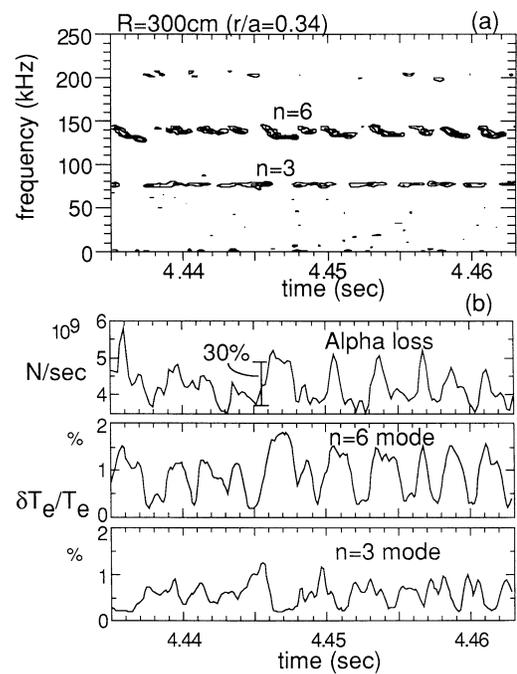

FIG. 3. The high frequency modes at the time t_2 in Fig. 1. (a) Same contour plot as Fig. 2(a). A bursting $n = 6$ mode is observed. (b) A very good correlation is observed between the enhanced alpha loss and the $n = 6$ mode. The $n = 3$ mode shows a negative correlation.

of 2 above the background level in the lost-α signal, Fig. 2(b). Here, the background loss is mainly from the first orbit loss [4], which is about 3% of the total alpha production rate. The measured escaping alpha particles have energy close to 3.5 MeV. Detailed correlation analysis shows that the enhanced α loss correlates mainly with the $n = 6$ and $n \geq 8$ modes. In another discharge where all the $n = 1-9$ modes are present, the enhanced loss only correlates with $n \geq 6$ modes. This seems to indicate that not all the MHD modes play the same role in the wave-particle interaction process even when they have the same location and comparable fluctuation amplitudes. Among the four alpha loss detectors located at different poloidal angles, 20°, 45°, 60°, and 90° below the outer midplane, the loss bursts can be seen in the bottom three detectors, but only the 90° detector shows the correlation described above. This correlation becomes much clearer in the following bursting mode case.

(2) Bursting mode.—Between the large loss bursts, the 90° detector also shows some lower level intermittent loss enhancement. It is found that these oscillations correlate very well with a bursting mode. Figure 3(a) shows the same δT_e frequency spectrum contour plot. Only two modes are observed with $n = 3$ and 6 (plus a very weak mode at ~ 200 kHz). These n numbers measured by the magnetic coils are verified by the phase correlation analysis between the two ECE grating arrays located 120° apart toroidally. In addition, the phase symmetry of the modes measured on the inner and outer mode locations indicates that both the $n = 6$ and $n = 3$ modes have even poloidal mode numbers (m).

The $n = 6$ mode is bursting in time. A drop of $\sim 14\%$ in mode frequency is also seen on each burst. It is somewhat analogous to the beam-ion-driven fishbone mode ($m = 1, n = 1$) routinely observed in TFTR neutral beam–heated supershots [7], except for having much higher mode numbers and frequency. Figure 3(b) shows the time evolution of the lost-α signal and the MHD modes. A very good correlation is observed between this bursting $n = 6$ mode and the alpha loss. Each burst corresponds to a $\sim 30\%$ enhancement in the α-loss signal at the 90° detector, or about 1% of the alpha birth rate. In contrast, the lower frequency $n = 3$ mode shows a negative correlation with the alpha loss. Since both of the modes appear at the same spatial location, this selective correlation is evidence of frequency-dependent wave-particle resonance.

The radial mode structure measured by the ECE system is shown in Fig. 4(a) for the $n = 6$ and $n = 3$ modes. A ballooning character is clearly seen in the $n = 6$ mode, i.e., the mode amplitude is stronger in the low B field side ($R > R_0$) than the high B field side. The maximum $\delta T_e/T_e$ is $\sim 2\%$. It corresponds to a local magnetic perturbation $\delta B_r/B_0 \sim (1/qR)|\delta T_e/\nabla T_e| \sim \mathcal{O}(10^{-4})$ (since $\mathbf{B} \cdot \nabla \sim B/qR$ for the ballooning mode). The bursting $n = 6$ mode is observed in three ECE channels. The channel-to-channel separation is about 5–6 cm, so the mode width is about $\delta r \lesssim 12$ cm or $\delta r/a \sim 0.14$. It covers $q \simeq 1.1-1.5$. In the multifrequency case the
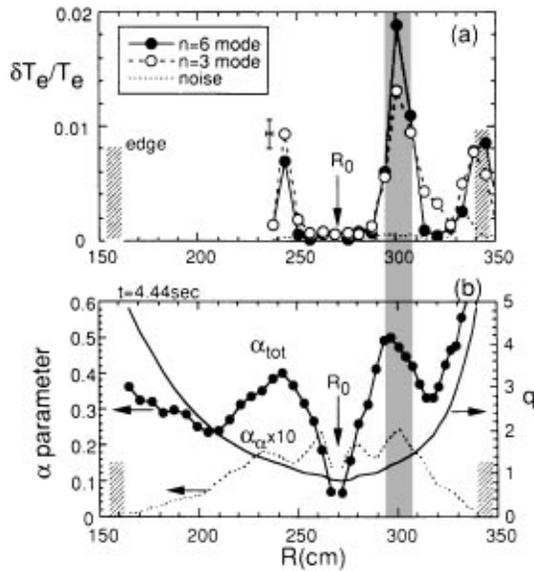
FIG. 4. (a) Radial profiles of $\delta T_e/T_e$ for the $n = 6$ and $n = 3$ modes. (b) Profiles of the α parameter defined in Eq. (1) and the safety factor q. The α_α is for the alpha particles. The MHD is located at the peak pressure gradient where $q \simeq 1.3$.

FIG. 5. (a) Orbit tracing of the lost-alpha particles. The measured pitch angle and the particle energy (~ 3.5 MeV) are used. (b) A cross-section projection of the alpha particle orbit from an orbit simulation code. The measured mode number ($m = 8$, $n = 6$), frequency (80 kHz in plasma frame), and radial profile are used. The initial energy is 3.08 MeV, pitch angle $v_\parallel/v = -0.55$.

high-n modes have a narrower width, i.e., $\delta r \sim 8$ cm or $\delta r/a \sim 0.09$. Using a transport analysis code (TRANSP [8]) we found that these modes are located at the peak value of α_{tot}; see Fig. 4(b). Here, α_{tot} is a measure of the plasma pressure gradient defined as

$$\alpha_{\text{tot}} = -R_0 q^2 d\beta_{\text{tot}}/dr, \qquad (1)$$

where β_{tot} is the total plasma toroidal beta (thermal plasma plus beam ions) and R_0 is the magnetic axis location. The safety factor profile is from a TRANSP calculation. The q value at the mode location is ~ 1.3. Therefore, the best helical mode numbers that match the even parity from the ECE measurement discussed above are, respectively, $m/n = 8/6$ and $m/n = 4/3$. This TRANSP q profile is also partly justified by the agreement between the $q = 1$ surface and the measured inversion radius of the minor disruption at 4.55 sec.

The mode frequency in the plasma frame can be calculated by subtracting out the toroidal rotation frequency, i.e.,

$$\omega_{\text{MHD}} = \omega_{\text{lab}} - \omega_{V_\phi}, \qquad (2)$$

where $\omega_{V_\phi} = (n/R)V_\phi$, n is the toroidal mode number, and R is the mode location. Using the $V_\phi(R)$ profile measured from a charge-exchange spectroscopy system, we find that $\omega_{V_\phi}(n = 6) \simeq 2\pi(47 \pm 5$ kHz). Therefore, the mode frequency in the plasma frame is $\omega_{\text{MHD}} \simeq 2\pi(88 \pm 5$ kHz).

(3) Particle loss simulation.— An alpha particle orbit lost to a detector can be traced back into the plasma by using the measured particle energy, pitch angle, and equilibrium parameters such as the q profile. Figure 5(a) shows such an orbit. We see that particles that escape to
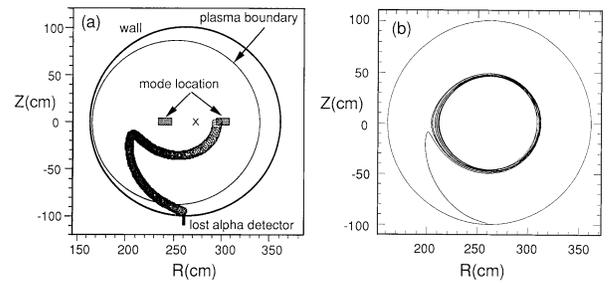
the 90° detector arrive on barely trapped banana orbits. The location of the high frequency mode is around the inner excursion of the banana orbit, which supports the physical assumption that the alpha particles are expelled by the MHD modes.

A guiding center code [9] was used to simulate the mode-induced particle loss. We use the experimentally observed parameters: $m = 8$, $n = 6$, $f = 80$ kHz and use $\delta B_r/B_0 = 2 \times 10^{-4}$. The particle distribution is a Monte Carlo generated alpha particle slowing-down distribution, isotropic in pitch angle, with a Gaussian radial profile taken to approximate the experimental conditions. An example of induced loss of the type seen by the detector is shown in Fig. 5(b). The lost particles are countermoving (opposite to the plasma current direction) passing particles initially located at a smaller minor radius. The wave-particle resonance condition in the plasma frame can be written as $n\phi - m_d\theta - \omega_{\text{MHD}}t = \text{const}$, where $m_d = m, m \pm 1$. For a countermoving passing particle, $\phi = -\omega_t t$, $\theta = -\omega_t t/q$, where $\omega_t \sim |v_\parallel|/R$ is the toroidal transit frequency. The resonant condition becomes

$$\omega_{\text{MHD}} \simeq (m_d/q - n)\omega_t. \qquad (3)$$

The case shown in Fig. 5(b) has a resonance with $m_d = 7$. The simulation shows that the particle spends only a small fraction of each poloidal transit in resonance when the orbit passes through the outer midplane. During each resonant period, it can gain or lose energy to the wave in a random walk process in $v_\parallel$ until it eventually diffuses into a trapped orbit. The total simulated alpha loss for a 1 msec burst of the mode is $\sim 1\%$ of the alpha particle population (with $E \sim 1.5-3.5$ MeV). On the other hand, a similar simulation shows that the $n = 3$ mode has less than half this effect due to lack of efficient wave-particle resonance. All these results are basically consistent with the observations. We have also simulated the effect of the mode on the beam population, but observe no losses. (No beam-ion loss measurement is available in routine TFTR experiments.)

(4) Linear stability analysis.—An MHD stability calculation for this discharge has also been carried out. First of all, we conclude that the observed high frequency modes are not the TAE (toroidicity-induced Alfvén eigenmodes) [10], because the TAE frequency is more than a factor of 2 higher.

Due to the strong local peaking of the pressure profile, it is found that the plasma at $r/a \sim 0.34$ has reached and even exceeded the high-n ideal ballooning limit at $t \simeq 4.2-4.55$ sec. This suggests that the mode we observed should be related to the ballooning modes, especially to the kinetic MHD ballooning mode (KBM) [11]. (Note that these modes are different from the ideal ballooning modes observed in TFTR before high-β disruptions [12], which are toroidally localized and have larger radial extent.) The basic characteristic of the KBM is that the mode frequency is close to the ion-diamagnetic frequency, i.e.,

$$\omega_{*pi}/2 < \omega_r < \omega_{*pi}, \tag{4}$$

where $\omega_{*pi} = (nq/r)(v_i^2/\Omega_i)d\ln p_i/dr$. The high frequency modes we observed are within this range [3]. For example, the $n = 6$ ion-diamagnetic frequency (using only the thermal ions) is $\sim$110 kHz, which is about $1.2\omega_{MHD}$.

A comprehensive kinetic calculation described in detail in Ref. [13] is employed to study the linear stability properties of the high-n MHD ballooning mode, using the so-called ballooning representation for high-n modes. This calculation is fully electromagnetic. It includes multiple ion species and kinetic effects from trapped and untrapped particles, finite Larmor radius, Landau damping, etc. Maxwellian equilibrium distribution functions are used for each of the eight plasma species (e, H, background D and T, impurity C, hot beam D and T, and hot α), except the hot alpha particles for which a slowing-down distribution is used. A finite-β numerically calculated MHD equilibrium based on experimentally measured profiles is employed.

The results for the linear growth rate γ vs r/a is shown in Fig. 6. The plasma is locally unstable to the KBM driven by the background pressure gradient. The effect of the hot beam species is slightly stabilizing for this case, while that of the hot alpha particles is slightly destabilizing. The spatial location of the KBM is in general agreement with the experiment. The linear growth rate has a maximum at $n = 14$ for $r/a = 0.34$, while the observed modes have lower values of n. However, we believe that nonlinear effects can downshift the peak of n [14].

In conclusion, a significant enhancement (from $\sim$30% to a factor of 2) in alpha particle loss correlated with high frequency MHD modes has been observed in recent TFTR high-β DT plasmas. Both the experimental measurements and particle simulation show that the observed alpha loss is induced by the wave-particle resonance between the alpha particles and the MHD modes (mainly,
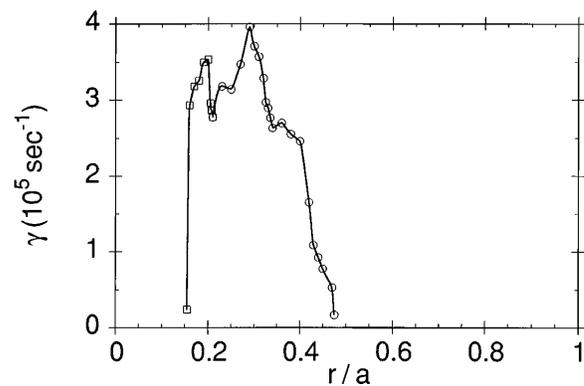

FIG. 6. Linear growth rate γ versus r/a for the kinetically calculated high-n MHD ballooning mode at $t = 4.40$ sec. Here, $k_{\theta\rho_D} \simeq 0.2-0.3$, the value which maximizes γ at $r/a = 0.34$.

the $n = 6$ mode). Linear stability analysis shows that the plasma is locally unstable to the KBM driven by the strong plasma pressure gradient. Although these modes seem unlikely to be driven by α particles (similar MHD activity is observed in D-only plasmas [3]), our observation indicates that the high frequency KBM modes can have significant effects on the fusion ion confinement in the high-β regime. Therefore, attention needs to be paid to the impact of these modes on future tokamak reactors.

[1] H. P. Furth *et al.,* Nucl. Fusion **30**, 1799 (1990).
[2] D. Mansfield *et al.,* Phys. Plasmas **2**, 4252 (1995).
[3] R. Nazikian *et al.* (to be published).
[4] S. J. Zweben *et al.,* Nucl. Fusion **31**, 2219 (1991).
[5] A. Janos *et al.,* Rev. Sci. Instrum. **66**, 668 (1995).
[6] E. Fredrickson *et al.,* Rev. Sci. Instrum. **57**, 2084 (1986).
[7] R. Kaita *et al.,* Phys. Fluids B **2**, 1584 (1990).
[8] R. V. Budny, Nucl. Fusion **34**, 1247 (1994), and references therein.
[9] R. B. White and M. S. Chance, Phys. Fluids **27**, 2455 (1984); R. B. White, Phys. Fluids B **2**, 845 (1990).
[10] C. Z. Cheng *et al.,* Ann. Phys. (N.Y.) **161**, 21 (1985).
[11] An incomplete list of references on the KBM theory: W. M. Tang *et al.,* Nucl. Fusion **20**, 1439 (1980); C. Z. Cheng Phys. Fluids **25**, 1020 (1982); J. Wieland and L. Chen, Phys. Fluids **28**, 1359 (1985); H. Biglari and L. Chen, Phys. Rev. Lett. **67**, 3681 (1991); S.-T. Tsai and L. Chen, Phys. Fluids B **5**, 3284 (1993).
[12] E. Fredrickson *et al.* (to be published).
[13] G. Rewoldt *et al.,* Phys. Fluids **25**, 480 (1982); G. Rewoldt *et al.,* Phys. Fluids **30**, 807 (1987).
[14] S. E. Parker *et al.,* Phys. Rev. Lett. **71**, 2042 (1993).